

Report on Visit to University of California, Los Angeles by International Training Program

Dept. of Electrical Engineering and Computer Science Nagoya University Hiroshi Yamamoto

This report is summary of my work in Prof. Chang's Laboratory of University of California, Los Angeles (UCLA). My research focused on plasma etch chemistry for metals and metal oxides, with an emphasis on thermodynamics.

Introduction of UCLA

UCLA is a public research university located in the Westwood neighborhood of Los Angeles, California, USA. It was founded in 1919 as the "Southern Branch" of the University of California and is the second oldest of the ten campuses. UCLA, considered as one of the flagship institutions of the University of California system, offers over 300 undergraduate and graduate degree programs in a wide range of disciplines and enrolls about 26,000 undergraduate and about 11,000 graduate students from the United States and around the world. Strengths in liberal arts, sciences and research earned it membership in the Association of American Universities [1]. Figure 1 is a picture of Royce hall, one of the landmarks of UCLA. The UCLA Chemical and Biomolecular Engineering Department was established in 1983. Despite its relative youth, the department has established itself as the primary supplier of B.S. chemical engineers in Southern California and as a research force to be reckoned with. Departmental offices are located in Boelter Hall, adjacent to Mathematical Sciences, and across the Science Quadrangle from the Department of Chemistry and Biochemistry. Approximately 70 chemical engineering graduate students are in residence, most of them pursuing Ph.D. degrees. Nearly all graduate students receive financial support either from research and teaching assistantships, or from internal or external fellowships. Teaching is viewed as an integral part of the graduate experience, and all graduate students participate in the instruction of approximately 275 undergraduates [2].



Fig. 1. Royce Hall, one of the landmarks of UCLA.



Fig. 2. Group dinner with Prof. Chang's Lab. Members (from left, Diana Chien, James Dorman, Ya-Chuan (Sandy) Perng, Han Chueh, Jack Chen, Dr. Ju Choi, Prof. Jane P. Chang, Calvin Pham, Jea Cho, Hiroshi Yamamoto, Nathan Marchack).

Background on Plasma Chemistry Selection

Metals and metal oxides have been used for a variety of kinds of electronics devices because of their electrical characteristics. This work addresses two applications: First is the patterning of High-k dielectric materials and second is the patterning of materials in magnetic tunnel junction in Spin-Transfer Torque Random Access Memory (STT-RAM).

A. High-k/Metal Gate Patterning Process

Semiconductor industry has been evolving based on Moore's law for scaling. The wafer size becomes larger for enhancing the device yield and cost-effective products. While individual device are miniaturized. Nowadays, serious problems have been reported with the increase in the density of transistors. One problem is the increase of leakage current on gate dielectric. Gate dielectrics, traditionally made with SiO₂, reached only a few molecular layers thick (around 1 nm). SiO₂ is ideally an insulator, but at this thickness, quantum tunneling causes unacceptably high leakage current. One of the promising ways for the reduction of the leakage current is the introduction of High-k dielectric and metal gate. Several metal oxides such as zirconium oxide, Aluminum oxide and Hafnium oxide have been suggested as the high-k dielectric. These metal oxides can be made thicker to suppress the leakage current. As in conventional devices, High-k/Metal gates need to be patterned and plasma etching is one alternative. The increase in the complexity of materials employed in the high-k gate stack further complicates the patterning step, as critical parameters such as etching selectivity to the gate material and substrate and plasma damage must be accounted for with a wide variety of material combinations.

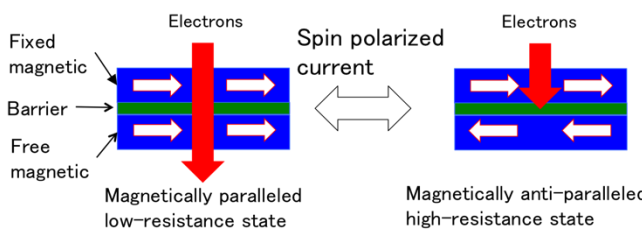


Fig. 3. Schematic representation of the TMR effect.

B. STT-RAM

There are many kinds of memory devices in use today, such as, static random access memory (SRAM) for cache memory in CPU, dynamic random access memory (DRAM) for main memory, and Flash memory is used for storage memory. Basically, there is a trade-off between performance and cost. For example, SRAM is the fastest and its endurance is very long, however, its capacity or integration is low, and power consumption is high. DRAM is also fast and its endurance is long but it needs refresh current to save data, which leads to high power consumption. On top of that, SRAM and DRAM are volatile memories, which means its stored information is lost if the power is removed. While Flash memory is a non-volatile memory, however, it has limited endurance, and its write speed is slow. STT-RAM is non-volatile, highly scalable, has high read/write speed (close to SRAM), a very long endurance and low power consumption. STT-RAM could potentially replace SRAM, DRAM, and Flash memory. As the same way DRAM stores the information by capacitors,

STT-RAM stores the information by Magnetic Tunnel Junction device (MTJ). MTJ consists of a free magnetic layer, a non-magnetic barrier layer, and a fixed magnetic layer as shown in Fig. 3. When the magnetic layers are magnetically parallel, a portion of the current passes through. This is equivalent to the low-resistance state. When the magnetic layers are magnetized antiparallel to each other, no portion of the current may pass through the stack without significant scattering, which is equivalent to a high-resistance state. This is called Tunneling Magnetoresistance (TMR) effect. These states are equivalent to "0" and "1". MTJ can store the information by changing the condition of free magnetic layer with spin-polarized current. STT-RAM utilizes a spin polarized current to switch the magnetization of a nanomagnet, which means switch "0" and "1". In a MTJ, the free and fixed magnetic layers are made with ferromagnetics such as CoFe, CoFeB and the non-magnetic barrier layer is made with metal oxide such as MgO, Al₂O₃.

C. Plasma Etching

The continued miniaturization of semiconductor devices dictates higher selectivity. Less damage in plasma patterning processes was investigated.

There are many challenges in etch noble metals and metal oxides. For instance, the melting point and boiling point of metal halide are relatively high and bond strength between the metal and oxygen are high as shown in Table 1 and 2. Some of them are etching-retardant materials [3].

To investigate plasma etch chemistry of metals and metal oxides, thermodynamic data have been used because thermodynamics is basic and essential data for understanding chemical processing. Volatility diagram is one of the applications of the thermodynamic data. The diagrams are typically used in the high temperature industry to examine volatility behavior of materials. In this work, it helps with the selection of etch chemistry.

Chlorine vs Fluorine Chemistry

Chlorine chemistry such as Cl_2 and BCl_3 [5-9] and fluorine chemistry such as CF_4 , C_4F_8 , and CHF_3 [11-13] have been suggested for high-k materials such as HfO_2 , and ZrO_2 because the volatilities of chlorides of Hf and Zr are relatively high and fluorine atom is a highly reactive species.

Table 3 and 4 show heats of reaction at room temperature for possible etching reaction of HfO_2 in Cl_2/BCl_3 plasma and fluorocarbon plasma, respectively, [3-5,14,15] where ΔH° are enthalpy of formation. F radicals have higher reactivity compared with Cl radicals. The reactions are more favorable when boron or carbon are present in plasma because of the reaction with and removal of oxygen. From the viewpoint of enthalpy for formation, in HfO_2 etching, Cl_2/BCl_3 chemistry has a higher reactivity due to strong bonding oxygen and boron chloride and relatively low boiling point of Hafnium chloride.

Table 1. Melting point and boiling point of metal halide.

Element	Halogen compound	Melting point (°C)	Boiling point (°C)
Al (Z = 13)	AlF_3	2250	1276
	AlCl_3	192.6	–
	AlBr_3	97.5	255
Si (Z = 14)	SiF_4	–90.2	–86
	SiCl_4	–68.85	57.65
	SiBr_4	5.2	154
Zr (Z = 40)	ZrF_4	–	912 sp
	ZrCl_4	–	331 sp
	ZrBr_4	–	360 sp
Hf (Z = 72)	HfF_4	–	970 sp
	HfCl_4	–	317 sp
	HfBr_4	–	323 sp

sp: sublimation point

Table 2. Bond strength of high-k materials related atoms.

Bond	Bond strength (eV)	Bond	Bond strength (eV)
B-O	8.38	Si-O	8.29
B-F	7.85	Si-F	5.73
B-Cl	5.30	Si-Cl	4.21
B-Br	4.11	Si-Br	3.81
		Si-Si	3.39
C-O	11.15	Zr-O	8.03
C-F	5.72	Zr-F	6.38
C-Cl	4.11	Zr-Cl	5.11
C-Br	2.90	Zr-Br	–
Al-O	5.30	Hf-O	8.30
Al-F	6.88	Hf-F	6.73
Al-Cl	5.30	Hf-Cl	5.16
Al-Br	4.45	Hf-Br	–

Table 3. Possible reaction in etching of HfO_2 in CF_4 plasma.

	ΔH° (kJ/mol)
$\text{HfO}_2(\text{s}) + 4\text{F}(\text{g}) \rightarrow \text{HfF}_4(\text{g}) + 2\text{O}(\text{g})$	-373.9
$\text{HfO}_2(\text{s}) + 4\text{CF}(\text{g}) \rightarrow \text{HfF}_4(\text{g}) + 2\text{CO} + 2\text{C}(\text{g})$	-331.8
$\text{HfO}_2(\text{s}) + 2\text{CF}_2(\text{g}) \rightarrow \text{HfF}_4(\text{g}) + 2\text{CO}(\text{g})$	-434.6
$\text{HfO}_2(\text{s}) + 2\text{CF}_3(\text{g}) \rightarrow \text{HfF}_4(\text{g}) + \text{CF}_2\text{O}(\text{g}) + \text{CO}(\text{g})$	-333.7
$\text{HfO}_2(\text{s}) + 2\text{CF}_3(\text{g}) \rightarrow \text{HfF}_4(\text{g}) + 2\text{CFO}(\text{g})$	68.5
$\text{HfO}_2(\text{s}) + 4\text{F}(\text{g}) + 2\text{CF}(\text{g}) \rightarrow \text{HfF}_4(\text{g}) + 2\text{CFO}(\text{g})$	-1709.0
$\text{HfO}_2(\text{s}) + 6\text{F}(\text{g}) + 2\text{CF}(\text{g}) \rightarrow \text{HfF}_4(\text{g}) + 2\text{CF}_2\text{O}(\text{g})$	-2793.2
$\text{HfO}_2(\text{s}) + 4\text{F}(\text{g}) + 2\text{CF}_2(\text{g}) \rightarrow \text{HfF}_4(\text{g}) + 2\text{CF}_2\text{O}(\text{g})$	-1798.6
$\text{HfO}_2(\text{s}) + 2\text{F}(\text{g}) + 2\text{CF}_2(\text{g}) \rightarrow \text{HfF}_4(\text{g}) + 2\text{CFO}(\text{g})$	-714.4
$\text{HfO}_2(\text{s}) + 2\text{F}(\text{g}) + 2\text{CF}_3(\text{g}) \rightarrow \text{HfF}_4(\text{g}) + 2\text{CF}_2\text{O}(\text{g})$	-1015.7

Table 4. Possible reaction in etching of HfO₂ in BCl₃ plasma

	ΔH° (kJ/mol)
$\text{HfO}_2(\text{s}) + 4\text{Cl}(\text{g}) \rightarrow \text{HfCl}_4(\text{g}) + 2\text{O}(\text{g})$	136.0
$\text{HfO}_2(\text{s}) + 6\text{Cl}(\text{g}) \rightarrow \text{HfCl}_4(\text{g}) + 2\text{ClO}(\text{g})$	-402.5
$\text{HfO}_2(\text{s}) + 6\text{BCl}(\text{g}) \rightarrow \text{HfCl}_4(\text{g}) + 2\text{BOCl}(\text{g}) + 2\text{B}(\text{g})$	-228.3
$\text{HfO}_2(\text{s}) + 4\text{Cl}(\text{g}) + 2\text{BCl}(\text{g}) \rightarrow \text{HfCl}_4(\text{g}) + 2\text{BOCl}(\text{g})$	-1277.8
$\text{HfO}_2(\text{s}) + 8\text{Cl}(\text{g}) + 4\text{BCl}(\text{g}) \rightarrow \text{HfCl}_4(\text{g}) + 2\text{B}_2\text{OCl}_4(\text{g})$	-3359.1
$\text{HfO}_2(\text{s}) + 6\text{Cl}(\text{g}) + 3\text{BCl}(\text{g}) \rightarrow \text{HfCl}_4(\text{g}) + \text{B}_3\text{O}_2\text{Cl}_5(\text{g})$	-2559.2
$\text{HfO}_2(\text{s}) + 4\text{Cl}(\text{g}) + 4\text{BCl}_2(\text{g}) \rightarrow \text{HfCl}_4(\text{g}) + 2\text{B}_2\text{OCl}_4(\text{g})$	-1973.5
$\text{HfO}_2(\text{s}) + 3\text{Cl}(\text{g}) + 3\text{BCl}_2(\text{g}) \rightarrow \text{HfCl}_4(\text{g}) + \text{B}_3\text{O}_2\text{Cl}_5(\text{g})$	-1520.1

However, perfluorocarbon gases such as CF₄ and C₄F₈ have high global warming potential values. Fluorocarbon molecules are strong absorbers of infrared radiation, which means they are powerful greenhouse gases. Their long lifetime (up to 50,000 years) due to its stability is also a major concern. Even though the atmospheric concentration of perfluoromethane is around 100,000 times lower than CO₂, the greenhouse warming potential of tetrafluoromethane and hexafluoroethane is 6,500 and 9,200 times that of carbon dioxide, respectively. [16,17] Several governments concerned about the properties of perfluorocarbon have already tried to implement international agreements to limit their usage before it becomes a global warming issue. The perfluorocarbons are one of the classes of compounds regulated in the Kyoto Protocol. From the viewpoint of chemistry and environment, chlorine chemistry is more adaptive than fluorine chemistry.

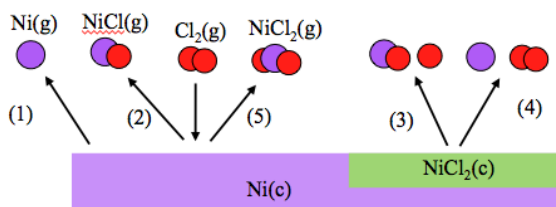


Fig. 4. Schematic representation of vaporization in Ni-Cl system.

Construction of Volatility Diagram for Ni-Cl System

Volatility diagrams are typically used in the high temperature industry to examine volatility behavior of materials such as refractories and ceramics when exposed to high temperatures and reactive environments [18-20].

In the volatility diagram for the Ni-Cl system, the partial pressures of the Ni-based gaseous species are shown as a function of the chlorine partial pressure at various temperatures. The relation between solid species and gas species can be determined from the thermodynamic equilibrium between the solid species and the gas species. Reactions involving only gases are ignored.

The equilibrium constant k is given by this equation, which relates with Gibbs free energy. The Gibbs energy and the other thermodynamic data can be obtained from the chemical database such as CRC Handbook and NIST-JANAF.

$$\log k = -\frac{DG^\circ}{RT} \quad (1)$$

where ΔG° is Gibbs free energy for the reaction, R is the universal gas constant, T is the absolute temperature, and k is the equilibrium constant for a reaction

Table 5 shows reactions and thermodynamic data for plotting volatility diagrams in Ni-Cl system. For instance, reaction 1 describe the vaporization of condensed Ni to Ni(g) and reaction 3 describe the vaporization of condensed NiCl₂ to NiCl(g) as shown in Fig. 4.

Table 5. Reactions for plotting volatility diagrams in Ni-Cl system.

Reaction	ΔH°	ΔG°	$\log(K) = -\Delta G^\circ/RT$
1 Ni(c) \rightarrow Ni(g)	430.1	384.7	-67.4 kJ/mol
2 Ni(c) + 1/2Cl ₂ (g) \rightarrow NiCl(g)	182.0	149.1	-26.1
3 NiCl ₂ (c) \rightarrow NiCl(g) + 1/2Cl ₂ (g)	486.9	407.8	-71.4
4 NiCl ₂ (c) \rightarrow Ni(g) + Cl ₂ (g)	735.0	643.5	-112.7
5 Ni(c) + Cl ₂ (g) \rightarrow NiCl ₂ (c)	-304.9	-258.8	45.3
6 NiCl ₂ (c) \rightarrow NiCl ₂ (g)	231.0	172.5	-30.2
7 Ni(c) + Cl ₂ (g) \rightarrow NiCl ₂ (g)	-73.9	-86.2	15.1

The first step in the construction of the volatility diagram is to determine the regions that contain the condensed phases. Based on the definition of the equilibrium constant, the partial pressure of Ni(g) can be obtained. The line can be obtained from the equilibrium constant as shown

$$\log(k_1) = \log \frac{P_{Ni(g)}}{a_{Ni(c)}} \quad \text{where } a_{Ni} = 1,$$

$$\log(P_{Ni}) = \log(k_1) \quad (2)$$

This reaction describe the vaporization of Ni(c) to Ni(g), which is independent of the partial pressure of chlorine. We can plot this result in a volatility diagram as a horizontal line. In a similar way, the partial pressure of each gas species, NiCl(g), NiCl₂(g), can be calculated. Figures 5 – 7 show volatility diagrams for the Ni-Cl system at 298 K where the gas phase species are considered individually: (5) Ni(g), (6) NiCl(g), and (7) NiCl₂(g).

Comparison of Volatility Diagrams for Ni, Fe, Co

The complete volatility diagram for the Ni-Cl system at 298K is shown in Fig. 8. This is a superposition of Fig. 5-7, with the dominant vapor pressure lines in solid. The dashed vapor pressure lines represent vapor species having vapor pressures smaller than the maximum equilibrium vapor pressure lines. The volatility diagram is divided into three regions. In region I, Ni(g) is the dominant species over Ni. This changes to NiCl₂(g) in region II. In a similar way, complete volatility diagrams are determined based on reactions summarized in Tables 6 and 7 for Fe-Cl and Co-Cl system. Figures 9 and 10 show the complete volatility diagram for the Fe-Cl and Co-Cl system at 298K. Figure 11 shows volatility diagram for Ni-Cl, Co-Cl, and Fe-Cl system at 298K. Figures 9 and 11 revealed gas phase of Fe₂Cl₆ has the highest vapor pressure in Cl₂ gas. On top of that, enthalpies of formation of following reactions are more negative than the other reactions.

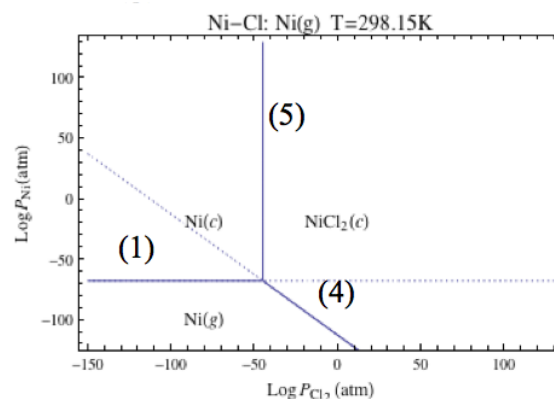


Fig. 5. Volatility diagram of Ni(g) for Ni-Cl system at 298K. (Partial pressures for all figures are given in atm (1 atm = 1.013 x 10⁵ Pa.)

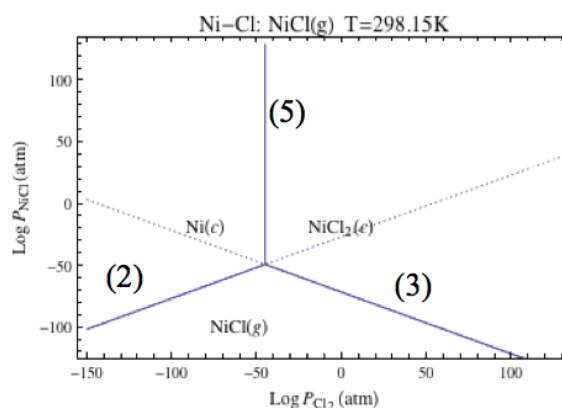


Fig. 6. Volatility diagram of NiCl(g) for Ni-Cl system at 298K.

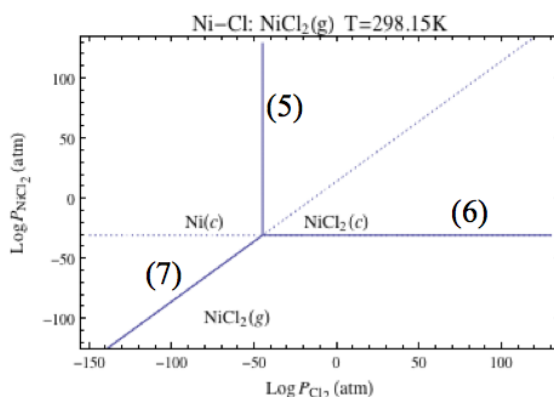
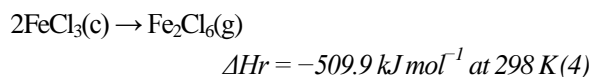
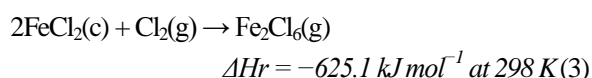


Fig. 7. Volatility diagram of NiCl₂(g) for Ni-Cl system at 298K.



These results indicate that the evaporation of Fe_2Cl_6 from FeCl_2 is more favorable and it is expected that iron can be etched chemically. In case of Ni and Co, the highest vapor pressures at room temperature are 10^{-30} and 10^{-20} at partial pressure between 0 and 1 atom, respectively.

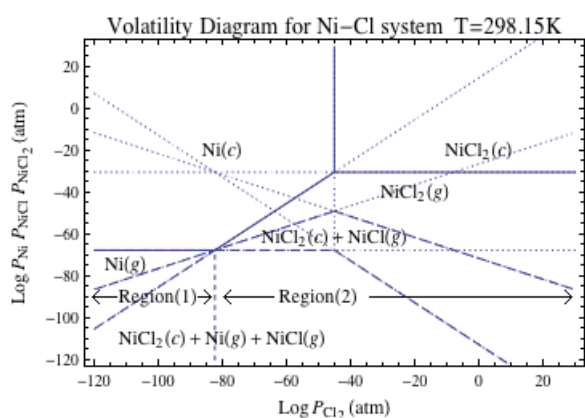


Fig. 8. Complete volatility diagram for the Ni-Cl system at 298K.

Table 6. Reactions for volatility diagrams in Fe-Cl system.

Reactions	ΔH° kJ/mol	$\log(k)$ kJ/mol	ΔG° kJ/mol
1 $\text{Fe}(\text{c}) + \text{Cl}_2(\text{g}) \rightarrow \text{FeCl}_2(\text{c})$	-341.8	53.0	-302.3
2 $\text{FeCl}_2(\text{c}) + 1/2\text{Cl}_2(\text{g}) \rightarrow \text{FeCl}_3(\text{c})$	-57.6	5.5	-31.6
3 $\text{Fe}(\text{c}) \rightarrow \text{Fe}(\text{g})$	415.5	-64.8	369.8
4 $\text{FeCl}_2(\text{c}) \rightarrow \text{Fe}(\text{g}) + \text{Cl}_2(\text{g})$	757.3	-117.7	672.1
5 $\text{FeCl}_3(\text{c}) \rightarrow \text{Fe}(\text{g}) + 3/2\text{Cl}_2(\text{g})$	814.9	-123.3	703.7
6 $\text{Fe}(\text{c}) + 1/2\text{Cl}_2(\text{g}) \rightarrow \text{FeCl}(\text{g})$	251.0	-37.8	215.6
7 $\text{FeCl}_2(\text{c}) \rightarrow \text{FeCl}(\text{g}) + 1/2\text{Cl}_2(\text{g})$	592.9	-90.7	518.0
8 $\text{FeCl}_3(\text{c}) \rightarrow \text{FeCl}(\text{g}) + \text{Cl}_2(\text{g})$	650.4	-96.3	549.6
9 $\text{Fe}(\text{c}) + \text{Cl}_2(\text{g}) \rightarrow \text{FeCl}_2(\text{g})$	-141.0	27.3	-155.6
10 $\text{FeCl}_2(\text{c}) \rightarrow \text{FeCl}_2(\text{g})$	200.8	-25.7	146.8
11 $\text{FeCl}_3(\text{c}) \rightarrow \text{FeCl}_3(\text{g}) + 1/2\text{Cl}_2(\text{g})$	258.4	-31.2	178.4
12 $\text{Fe}(\text{c}) + 3/2\text{Cl}_2(\text{g}) \rightarrow \text{FeCl}_3(\text{g})$	-253.1	43.4	-247.8
13 $\text{FeCl}_2(\text{c}) + 1/2\text{Cl}_2(\text{g}) \rightarrow \text{FeCl}_3(\text{g})$	88.7	-9.5	54.5
14 $\text{FeCl}_3(\text{c}) \rightarrow \text{FeCl}_3(\text{g})$	146.3	-15.1	86.1
15 $2\text{Fe}(\text{c}) + 3\text{Cl}_2(\text{g}) \rightarrow \text{Fe}_2\text{Cl}_6(\text{g})$	-1308.8	209.7	-1197.3
16 $2\text{FeCl}_2(\text{c}) + \text{Cl}_2(\text{g}) \rightarrow \text{Fe}_2\text{Cl}_6(\text{g})$	-625.1	103.8	-592.6
17 $2\text{FeCl}_3(\text{c}) \rightarrow \text{Fe}_2\text{Cl}_6(\text{g})$	-509.9	92.7	-529.4

Table 7. Reactions for volatility diagrams in Co-Cl system.

Reactions	ΔH° kJ/mol	$\log(k)$ kJ/mol	ΔG° kJ/mol
1 $\text{Co}(\text{c}) + \text{Cl}_2(\text{g}) \rightarrow \text{CoCl}_2(\text{c})$	-312.5	47.2	-269.6
2 $\text{Co}(\text{c}) \rightarrow \text{Co}(\text{g})$	426.7	-66.9	382.1
3 $\text{CoCl}_2(\text{c}) \rightarrow \text{Co}(\text{g}) + \text{Cl}_2(\text{g})$	739.2	-114.2	651.8
4 $\text{Co}(\text{c}) + 1/2\text{Cl}_2(\text{g}) \rightarrow \text{CoCl}(\text{g})$	192.9	-28.4	161.9
5 $\text{CoCl}_2(\text{c}) \rightarrow \text{CoCl}(\text{g}) + 1/2\text{Cl}_2(\text{g})$	505.4	-75.6	431.5
6 $\text{Co}(\text{c}) + \text{Cl}_2(\text{g}) \rightarrow \text{CoCl}_2(\text{g})$	-93.7	18.8	-107.2
7 $\text{CoCl}_2(\text{c}) \rightarrow \text{CoCl}_2(\text{g})$	218.8	-28.4	162.4
8 $\text{Co}(\text{c}) + 3/2\text{Cl}_2(\text{g}) \rightarrow \text{CoCl}_3(\text{g})$	-163.6	27.1	-154.5
9 $\text{CoCl}_2(\text{c}) + 1/2\text{Cl}_2(\text{g}) \rightarrow \text{CoCl}_3(\text{g})$	149.0	-20.2	115.1
10 $2\text{Co}(\text{c}) + 2\text{Cl}_2(\text{g}) \rightarrow \text{Co}_2\text{Cl}_6(\text{g})$	-350.6	58.5	-334.0
11 $2\text{CoCl}_2(\text{c}) \rightarrow \text{Co}_2\text{Cl}_6(\text{g})$	274.5	-36.0	205.3

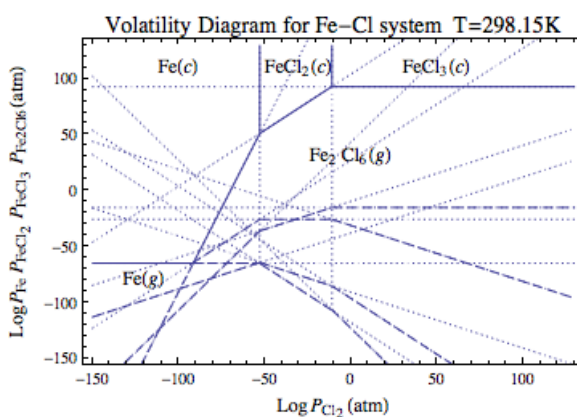


Fig. 9. Complete volatility diagram for the Fe-Cl system at 298K.

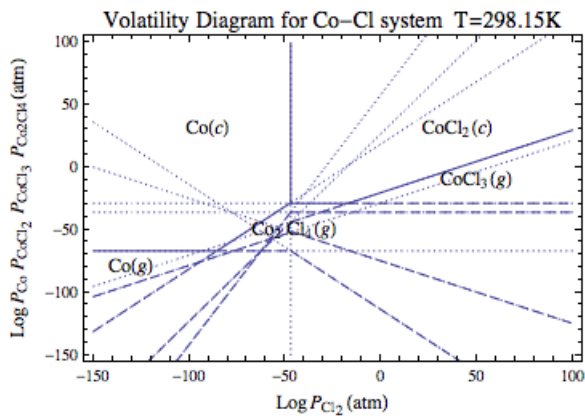


Fig. 10 Complete volatility diagram for the Co-Cl system at 298K.

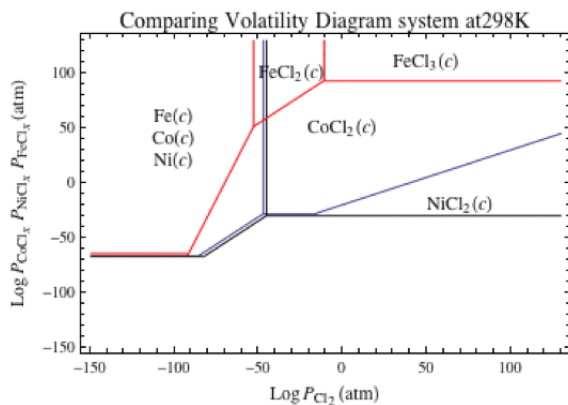


Fig. 11. Comparison of volatility diagram for Ni-Cl, Co-Cl, and Fe-Cl system at 298K.

Conclusion

Chemistry of plasma etching for metals and metal oxides were investigated and the volatility diagrams for Ni-Cl, Co-Cl, and Fe-Cl at room temperature were constructed in this work. Examination of the volatility diagrams revealed that gas phase of Fe_2Cl_6 has the highest vapor pressure in Cl_2 gas. Since the existence of the other kind of gases or radicals affect the volatility, the etch chemistry should be considered carefully. However, since enthalpies of formation of evaporation of Fe_2Cl_6 from FeCl_2 are negative. It can be expected that iron etching can be achieved by Cl_2 plasma. To etch Ni and Co, the other chemistry such as Cl_2/Ar [21,22] or NH_3/CO [23] chemistry should be considered.

Acknowledgements

I would like to first thank Prof. Chang for the opportunity to study in her group. Her guidance, valuable advices allowed me to progress in my understanding of this research. I would like to deeply thank Nathan Marchack for collaborating and giving valuable advices. A big thanks to members of Prof. Chang's group.

I believe that every experience that I've had in this program will help promote my future study in Japan. I also really appreciate Prof. Hiroataka Toyoda for supporting this program, Ms Mitsuko Era for helping me on lots of paper work for this program. Prof. Hori, Prof. Sekine, and Prof. Ishikawa for assisting my work during, without their support I could not finish this program.

This program was supported by International Training Program organized by Japan Society for the Promotion of Science.

References

- [1] Wikipedia (http://en.wikipedia.org/wiki/University_of_California,_Los_Angeles)
- [2] UCLA chemical and biomolecular engineering (<http://www.chemeng.ucla.edu/about/about-us>)
- [3] Handbook of Chemistry and Physics, 85th ed., edited by D. R. Lide (CRC, Boca Raton, FL, 2004).
- [4] R. M. Martin and J. P. Chang, J. Vac. Sci. Technol. A **27**, 217 (2009)
- [5] L. Sha and J.P. Chang, J. Vac. Sci. Technol. A **21**, 1915 (2003).
- [6] L. Sha, B.O. Cho and J.P. Chang, J. Vac. Sci. Technol. A **20**, 1525 (2002).
- [7] S. Norasetthekul, P.Y. Park, K.H. Baik, K.P. Lee, J.H. Shin, B.S. Jeong, V. Shishodia, D.P. Norton and J. Pearton, Appl. Surf. Sci. **187**, 75 (2002).
- [8] K. Nakamura, T. Kitagawa, K. Osari, K. Takahashi and K. Ono, Vacuum **80**, 761 (2006).
- [9] T. Kitagawa, K. Nakamura, K. Osari, K. Takahashi, K. Ono, M. Oosawa, S. Hasaka and M. Inoue, Jpn. J. Appl.

Phys. 45, L297 (2006).

[10] T. Maeda, H. Ito, R. Mitsuhashi, A. Horiuchi, T. Kawahara, A. Muto, T. Sasaki, K. Torii and H. Kitajima, *Jpn. J. Appl. Phys.* 43, 1864, (2004).

[11] J. Chen, W.J. Yoo, Z.Y. Tan, Y. Wang and D.S. H. Chan, *J. Vac. Sci. Technol. A* 22, 1552 (2004).

[12] K. Takahashi, K. Ono and Y. Setsuhara, *J. Vac. Sci. Technol. A* 23, 1691 (2005).

[13] K. Takahashi and K Ono, *J. Vac. Sci. Technol. A* 24, 437 (2006).

[14] B.O. Knacke, and O. Kubaschewski, *Thermochemical Properties of Inorganic Substances* (Springer-Verlag, Berlin, 1977).

[15] MOPAC

[16] A. M, Khalil K, Rasmussen RA, et al. (October 2003). "Atmospheric perfluorocarbons". *Environ. Sci. Technol.* 37 (19): 4358–61. doi:10.1021/es030327a. PMID 14572085.

[17] Environmental Protection Agency (19 Oct 2006). "High GWP Gases and Climate Change".

[18] N.S. Kulkarni, R.T. DeHoff, *J. Electrochem. Soc.*, 149, G620 (2002).

[19] C. Wagner, *J. Appl. Phys.*, 29, 1295 (1958).

[20] V. L. K. Lou, T. E. Mitchell, and A. H. Heuer, *J. Am. Ceram. Soc.*, **68**,49 (1985).

[21] K. B. Jung, H. Cho, Y. B. Hahn, D. C. Hays, T. Feng, Y. D. Park, J. R. Childress, and S. J. Pearton, *Materials Science and Engineering B* **60**, 101 (1999).

[22] H Cho, K Jung, D Hays, Y Hahn, T Feng, Y Park, J Childress, F Cadieu, R Rani, and X Qian, *Materials Science and Engineering B* **60**, 107 (1999).

[23] Jong-Yoon Park, Se-Koo Kang, Min-Hwan Jeon, Myung S. Jhon, and Geun-Young Yeom, *Journal of The Electrochemical Society* **158**, 1 (2011).

